JOURNAL OF AGRICULTURAL AND FOOD CHEMISTRY

J. Agric. Food Chem. **2004,** *52,* 5717−5723 **5717**

Effects of Designed Sulfhydryl Groups and Disulfide Bonds into Soybean Proglycinin on Its Structural Stability and Heat-Induced Gelation

MOTOYASU ADACHI, HO CHUNYING, AND SHIGERU UTSUMI*

Laboratory of Food Quality Design and Development, Graduate School of Agriculture, Kyoto University, Uji, Kyoto 611-0011, Japan

The gel-forming ability of glycinin is one of soybean's most important functional properties. The proglycinin A1aB1b homotrimer was engineered to introduce sulfhydryl groups and disulfide bonds, and their effects on the structural stability and the heat-induced gelation were evaluated. On the basis of the crystal structure, five mutants were designed and prepared: R161C and F163C forming an interprotomer disulfide bond with the inherent free cysteine residue of Cys377, N116C/P248C forming a new intraprotomer disulfide bond, and N116C and P248C introducing a new sulfhydryl group. Mutants of R161C, F163C, and N116C/P248C formed a new disulfide bond as expected. N116C/P248C was significantly more stable than the wild type against chemical and thermal denaturation and more resistant to α-chymotrypsin digestion, whereas F163C showed significantly increased thermal stability. All mutants exhibited greater hardness of heat-induced gels than wild type, and in particular, N116C/P248C gave the hardest gel. This result indicates that it is possible to increase hardness of glycinin gel by introduction of cysteine residues using protein engineering.

KEYWORDS: Gelation; mutant; proglycinin; soybean; structural stability

INTRODUCTION

The soybean is one of the most important food protein resources. The applicability of soybean proteins in foods is based on their functionality such as gelation, emulsification, foaming, etc. (*1*). Soybean proteins are composed of two major components, glycinin (11S globulin) and β-conglycinin (7S globulin), which account for about 40 and 30% of the total seed proteins, respectively. They are important determinants of functional properties of soybean proteins. Constituent subunits of glycinin have two or three disulfide bonds, whereas those of β-conglycinin have no disulfide bond (*1*). The five major subunits of glycinin have been identified as A1aB1b, A2B1a, A1bB2, A3B4, and A5A4B3 (*1*, *2*). In the cell, the constituent subunits are synthesized as a single polypeptide precursor. The signal sequence is removed cotranslationally, and proglycinin assembles into a trimer in the endoplasmic reticulum. As proglycinin is sorted to protein storage vacuoles, a specific post-translational cleavage occurs between asparagine and glycine residues, resulting in a mature subunit consisting of acidic and basic chains (*3*, *4*). Finally, glycinin assembles into a hexamer. Recently, we have solved crystal structures of proglycinin A1aB1b homotrimer (*5*) and the mature glycinin A3B4 homohexamer (*6*). These studies are useful in the improvement of the functional properties of glycinin based on structural coordinates.

* Corresponding author. Tel: +81-774-38-3760. Fax: +81-774-38-3761. E-mail: sutsumi@kais.kyoto-u.ac.jp.

The protomer structure of glycinin contains two β-barrel domains and two extended helix domains. Glycinin subunits have five variable regions based on their amino acid sequences (*7*, *8*), and these roughly correspond to the disordered regions in the crystal structure (*5*). Two disulfide bonds, which are conserved among 11S globulins from various legume and nonlegume seeds, were clearly confirmed in the crystal structures of both A1aB1b and A3B4 subunits (*5*, *6*). One is an intrachain disulfide bond (between Cys12 and Cys45 in A1aB1b subunit), and the other is an interchain disulfide bond (between Cys88 in the acidic chain and Cys298 in the basic chain in the case of A1aB1b subunit). We termed the two faces perpendicular to the 3-fold axis in the trimer as IA and IE faces (*5*). The IE and IA faces contain the interchain and intrachain disulfide bonds, respectively. The crystal structure of the A3B4 homohexamer shows that hexamerization is conducted by face-to-face stacking of IE faces between two trimers and suggests the movement of mobile disorder region IV, which covers the IE face in a proform, to the side of the trimer after the post-translational processing (*6*).

The gel-forming ability of the soybean proteins is one of its important functional properties (*1*). Glycinin has the ability to form heat-induced gels (*9*, *10*). Mori et al. demonstrated the ability of glycinin to form soluble aggregates in the gelation process and proposed the overall scheme of heat-induced change depending on protein concentration (*9*). In addition, the soluble aggregates and gel network were visualized by electron microscopy (*11*). To investigate the molecular forces involved in

10.1021/jf0496595 CCC: $27.50
Published on Web 08/14/2004

the gelation process, the effects of salt, reducing agents, denaturants, and water-miscible solvents on the heat-induced gelation have been studied (*4*, *12*). Nakamura et al. found that *N*-ethylmaleimide, a blocking agent of sulfhydryl groups, inhibited the gel formation of 5% glycinin solution, suggesting that the intermolecular disulfide exchange reaction may participate in the formation and branching of strands before the network formation in the gelation process (*11*).

Protein engineering is a powerful method to improve the functional properties of food proteins. Lee et al. reported the enhanced gelation characteristics of recombinant bovine β-lactoglobulin by the introduction of cysteine residues (*13*). In this study, five mutants were prepared by protein engineering to improve the gel-forming ability of proglycinin A1aB1b. Two mutants, R161C and F163C, were designed to introduce interprotomer disulfide bonds with the inherent free cysteine residue Cys377. Another mutant N116C/P248C was designed to add the intraprotomer disulfide bond. Two mutants, N116C and P248C, have an additional free cysteine residue.

MATERIALS AND METHODS

Site-Directed Mutagenesis. To construct expression plasmids for the mutants, site-directed mutagenesis on the cloned A1aB1b glycinin subunit in pET-21d vector (*14*) was achieved by using PCR. The primers used were for R161C: 5′-CGACCAGATGCCTTGCAGATTCTATCTTG-3′ and 5′-GCTGGTCTACGGAACGTCTAAGATAGAAC-3′; for F163C: 5′-GATGCCTAGGAGATGCTATCTTGCTGGG-3′ and 5′-CTACGGATCCTCTACGACGTCTAAGATAGAAC-3′; for N116C: 5′-CCAGAAGATCTATTGCTTCAGAGAGGGTG-3′ and 5′-GGTCTTCTAGATAACGAAGTCTCTCCCAC-3′; and for P248C: 5′-GAGCGTGATAAAATGCCCCACGGACGAGC-3′ and 5′-CTCGCACTATTTTACGGGGTGCCTGCTCG-3′. Plasmid template was amplified by 30 cycles of denaturation at 95 °C for 20 s, annealing at 58 °C for 30 s, and elongation at 68 °C for 10 min using Pfu DNA polymerase (Strategene) and Gene Amp 2400 (PerkinElmer). The products were phosphorylated and blunted. Then, they were ligated and transformed into *Escherichia coli* HB101 strain. The sequences of the coding region were confirmed by using ABI Prism 373 DNA sequencer (PerkinElmer/Applied Biosystems).

Protein Expression. The expression plasmids were transformed into *E. coli* AD494(DE3). One milliliter of an overnight culture was inoculated in 500 mL of LB medium containing 50 μg/mL carbenicillin and 15 μg/mL kanamycin and incubated at 37 °C until an OD_{600} of about 0.60. At this point, isopropyl-β-D-thiogalactopyranoside (IPTG) was added to a final concentration of 1 mM. The proteins were expressed by incubating the culture at 25 °C for 20 h. The cells were harvested by centrifugation at 6700*g* using an RPR9-2 rotor (Hitachi, Japan).

Protein Extraction and Purification. The recombinant proteins were extracted from *E. coli* cells by sonication. Extracts were subjected to ammonium sulfate fractionation. The fractions of 35−60% saturation containing recombinant proteins were dialyzed and subsequently applied on a Q-Sepharose HR column (Amersham Pharmacia Biotech). The recombinant proteins were eluted by a linear gradient of NaCl (0.15−0.40 M). The fractions containing recombinant proteins were pooled and further purified by applying on Hi-Prep 16/60 Sephacryl S-200 HR column (Amersham Pharmacia Biotech). Except when the NaCl concentration was specified, the buffer used in extraction and purification procedures was 35 mM potassium phosphate buffer (pH 7.6), 0.4 M NaCl, 1 mM EDTA, 10 mM 2-mercaptoethanol, 0.1 mM (*p*-amidinophenyl)methanesulfonyl fluoride (APMSF), 1 μg/mL pepstatin A, and 1 μg/mL leupeptin (buffer A).

SDS−PAGE Analysis under Reduced and Nonreduced Conditions. For reduced condition, 50 μL of protein solution was mixed with 50 μL of 2 ± SDS buffer containing 125 mM Tris (pH 6.8), 4% SDS, 0.2 M 2-mercaptoethanol, 18% glycerol, and 0.01% Bromophenol Blue. The mixed solution was loaded on 11% polyacrylamide gel (*15*). For nonreduced condition, iodoacetoamide was added to the protein solution after purification at a final concentration of 10 mM and was mixed with the 2 ± SDS buffer without 2-mercaptoethanol. The mixed solution was loaded on 7.5% polyacrylamide gel containing 6 M urea. Program Scion Image (Scion) was used for densitometric analysis.

Ellman Method. Modified Ellman reagent was prepared by dissolving 39.6 mg of 5,5′-dithio-bis(2-nitrobenzoic acid) (DTNB) in 10 mL of 0.05 M potassium phosphate buffer (pH7.6) (*16*, *17*). A 1 mL solution of 35 mM potassium phosphate buffer (pH 7.6) containing 0.2 mg of protein and 0.2% SDS was mixed with 8 μL of Ellman reagent. The color was allowed to develop, and the absorbance taken at 0, 2, 5, 15, and 20 min. The molar concentration of sulfhydryl groups in the protein was quantified at 412 nm using a molar absorptivity of 13 600 M^{-1} cm^{-1}. The protein contents of samples were determined using the Bradford method (*18*) with bovine serum albumin as a standard.

Differential Scanning Calorimetry (DSC) Analysis. DSC analysis was conducted using 1 mg/mL protein solution in 35 mM sodium phosphate buffer (pH 7.6), 0.4 M NaCl, 1 mM EDTA, 0.02% NaN_3, 0.1 mM *p*-APMSF, 1 mg/L pepstatin A, and 1 μg/mL leupeptin (μ = 0.5). Scanning was recorded using Microcal MC-2 Ultra Sensitive Microcalorimeter (Micro Cal Inc., Northampton, MA) at a rate of 1 deg/min.

Chemical Denaturation. Fluorescence spectra of samples at a concentration of 0.1 mg/mL in buffer A were analyzed at 25 °C using an F-300 spectrophotometer (Hitachi, Japan). After 30 min, incubation with different concentrations of guanidine hydrochloride (from 0 to 5 M) emission spectra was recorded at an excitation wavelength of 284 nm. The slit width was 5 nm for measuring excitation emission, and the scan rate and response were 60 nm/min and 0.5 s, respectively. The three constants $\Delta G(H_2O)$, m, and C_m were calculated from chemical denaturation experiments based on linear extrapolation method (*19*, *20*) using the program KaleidaGraph (HULINKS) in curve fitting. C_m is the concentration at which folded and unfolded molecules exist equivalently, m is a measure of the dependence on denaturant concentration, and $\Delta\Delta G$ is $[\Delta G(H_2O)\text{mutant} - \Delta G(H_2O)\text{WT}]^1$; $\Delta G(H_2O)$ is an estimate of the conformational stability of a protein at 0 M denaturant.

α-Chymotrypsin Digestion Analysis. The samples were dialyzed against 35 mM sodium phosphate buffer. Ten microliters of 0.1 mg/mL α-chymotrypsin (40 units/mg, Sigma-Aldrich) was mixed with 90 μL of 0.5 mg/mL protein sample. The mixtures were allowed to react at different times from 1 to 60 min at 25 °C. Ten microliters of buffer instead of enzyme solution was used to serve as a control. The digestion was terminated by boiling for 5 min and then immediately dipped and kept in ice water for another 5 min. SDS−PAGE was conducted, and the degree of the digestion that had occurred was measured. The two kinetic constants k_1 and k_2 of the α-chymotrypsin digestion were calculated based on the kinetic model proposed previously (*21*) using the program KaleidaGraph (HULINKS) in curve fitting. The value of k_1 denotes the rate of disappearance of the original protein per minute, while k_2 denotes the rate of disappearance of the major digestion product of 43 kDa per minute due to further band cleavage.

Heat-Induced Gelation. Protein solutions were dialyzed against 10 mM sodium phosphate buffer (pH 7.6) containing 1 mM EDTA, 0.1 mM *p*-APMSF, 1 μg/mL pepstatin A, and 1 μg/mL leupeptin at room temperature. The dialyzed solution was concentrated using Centriprep Centrifugal Filter Units and Microcon Centrifugal Filter Units (Millipore). After adjustment to the desired protein concentration, 10 μL of each sample was carefully pipetted into PCR tubes (0.2 mL Eppendorf tubes). The samples were then centrifuged using a swing rotor at 8000*g* for 5 min. Then, 20 μL of Nujol mineral oil was layered onto each protein solution, and the samples were again centrifuged under the same condition as before. The 0.2 mL plastic tubes including the 10 μL protein solutions under the oil at room temperature were quickly put on a Gene Amp 2400 (PerkinElmer) preincubated at 100 °C as a heating block and kept heated for 30 min. After heating, samples were cooled immediately to 20 °C and kept for more than 30 min in Gene Amp 2400. The hardness of the gel was measured at 20 °C using REONER RE-3305 (Yamaden, Japan). The plunger of 1 mm diameter was

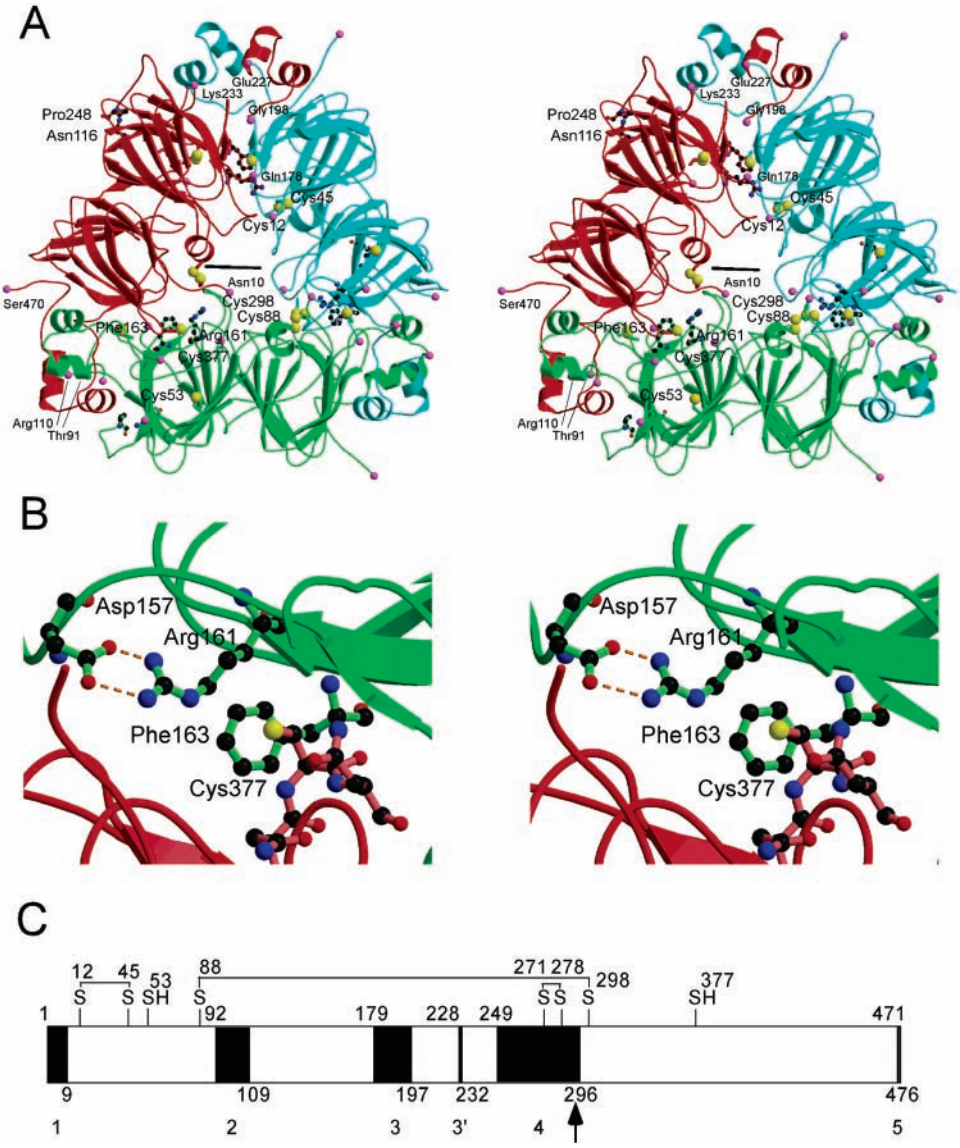

Figure 1. Stereoviews of the ribbon diagram. (**A**) Three protomers in the proglycinin trimer are shown in green, red, and cyan, respectively. The sulfur atoms in the cysteine residues forming disulfide bonds and in free cysteine residues are represented by yellow spheres with a radius of 1.2 Å. Six cysteine residues are labeled in the trimer: Cys53 in green protomer; Cys377 in red protomer; and Cys12, Cys45, Cys88, and Cys298 in cyan protomer. Four mutated residues of Asn116, Arg161, Phe163, and Pro248 are represented by ball-and-stick model. Arg161 and Phe163 are labeled in the green protomer, and Asn116 and Pro248 are labeled in the red protomer. The 3-fold symmetry axis is indicated by a black line at the center of the trimer. The disordered region 4 including the variable region VI is located between Pro248 and Ile297. (**B**) Magnified view of the structure around Cys377 is shown. Cys377 residue is located in the interface between two protomers shown in green and cyan. Asp157, Agr161, Phe163, and Cys377 are represented by ball-and-stick model. Carbon, nitrogen, oxygen, and sulfur atoms are shown in dark gray, blue, red, and yellow, respectively. Dotted orange lines indicate hydrogen bond. The model in panels A and B was generated using the programs MOLSCRIPT (*31*) and Rastor3D (*32*). (**C**) Schematic representation of proglycinin A1aB1b subunit is shown. Open and closed boxes represent modeled and disordered region, respectively (*5*). Numerals 1–5 at the bottom indicate disordered region. The arrow indicates the processing site responsible to separate acidic and basic chains between Asn291 and Gly292.

controlled at a speed of 1 mm/s and was stabbed into the gel of about 2 mm in height. Three samples were measured under the same conditions.

RESULTS AND DISCUSSION

Molecular Design of Proglycinin A1aB1b with Engineered Sulfhydryl Groups and Disulfide Bonds. Proglycinin A1aB1b subunit contains eight cysteine residues (*1*). The crystal structure of proglycinin A1aB1b homotrimer showed two disulfide bonds of Cys12−Cys45 and Cys88−Cys298 and two free cysteine residues of Cys53 and Cys377 (*5*) (**Figure 1**A,B). The remaining two cysteine residues are located in variable region IV disordered in the crystal structure and are believed to form disulfide bonds (*1*). Glycinin and other 11S globulins do not have an interprotomer disulfide bond. Cys377 is positioned on the interface between protomers in the molecule far from the solvent. **Figure 1B** shows the structure near the Cys377 residue. On the basis of the structure and two kinds of distance between Cα atoms and between Cβ atoms, it is possible that either of the two residues of Arg161 and Phe163, when replaced with cysteine residue, will form a disulfide bond with the Cys377 residue. The distances between Cα atoms and between Cβ atoms should be from 4.4 to 6.8 Å and from 3.5 to 4.5 Å, respectively (*22*, *23*). In fact, in the case of Arg161, the distances between Cα atoms and between Cβ atoms are 6.7 and 4.2 Å, respectively, whereas in the case of Phe163, the distances are 4.5 and 4.7 Å,

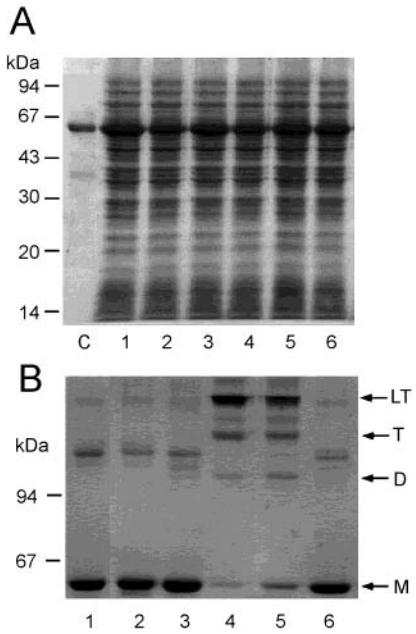

Figure 2. SDS–PAGE analyses for (**A**) expression level of WT and mutants and (**B**) interprotomer disulfide bond. SDS–PAGE were performed in the presence (**A**) and absence (**B**) of 2-mercaptoethanol. (**C**) Purified WT; 1, WT; 2, N116C; 3, P248C; 4, R161C; 5, F163C; and 6, N116C/P248C. M, D, T, and LT indicate monomer, dimer, trimer, and looped trimer, respectively.

respectively (*5*). There is no cysteine residue near Arg161 and Phe163 with the exception of Cys377. This manipulation resulted in the mutants R161C and F163C. On the other hand, we designed a new intraprotomer disulfide bond by introducing two cysteine residues in addition to the intrinsic disulfide bonds of Cys12−Cys45 and Cys88−298. We considered that two cysteine residues should not be near these intrinsic disulfide bonds on the primary and three-dimensional structures to avoid any incorrect formation of disulfide bond. Here, Asn116 and Pro248 were selected since the region from Cys88 and Cys271 is the longest region that does not contain any cysteine residue, and there is no disulfide bond at the N-terminal side of variable region IV, while Cys88−Cys298 is located at its C-terminal. Although the distances between Cα atoms and between Cβ atoms are 6.7 and 6.2 Å, it is expected that the disulfide bond of Cys116−Cys248 will be formed because the flexibility of Pro248 must be high since it is positioned just before the disordered region (resulting in the mutant N116C/N248C). Moreover, N116C and P248C were also constructed as mutants involving an additional sulfhydryl group. The introduced additional sulfhydryl group is not located near the intrinsic disulfide bonds on the primary and three-dimensional structures.

Expression and Purification of Proglycinin A1aB1b Mutants. Production of proglycinin mutants was assessed by SDS−PAGE using 11% acrylamide gel (**Figure 2**). The molecular sizes of all the expressed proteins were the same as that of the WT as expected. According to the densitometric analysis, the accumulation level of WT in the soluble fraction is calculated as 14%, and the ratio of N116C, P248C, R161C, F163C, and N116C/P248C to WT stands at 0.75, 0.92, 0.70, 0.99, and 0.76, respectively. The accumulation levels of N116C, R161C, and N116C/P248C were significantly lower than that of WT, whereas the accumulation levels of P248C and F163C were close to that of WT. Probably this is because the folding efficiency of N116C, R161C, and N116C/P248C for correct conformation is different from that of WT due to thiol−disulfide exchange reactions. It appears that the replacement of Asn116 with Cys116 will not affect properties such as solubility and interactions with surrounding residues because Asn116 is exposed to the solvent. Thus, Cys116 could only affect folding by the formation of an incorrect disulfide bond with Cys53 and Cys88 since their residues are located near the Cys116 residue from two points of view based on primary sequence and three-dimensional structure. On the other hand, the Arg161 residue is buried in the protein molecule and forms a salt bridge with Asp157. The replacement of Arg161 with Cys161 leaves Asp157 inside the protein molecule without a counterion. This may therefore affect its protein folding.

Table 1. Colorimetric Analysis by Ellman Method

protein	WT	N116C	P248C	R161C	F163C	N116C·P248C
no. of SH[a]	2	3	3	1	1	2
no. of SS (intra)[b]	3	3	3	3	3	4
no. of SS (inter)[c]	0	0	0	1	1	0
no. of SH (Ellman)[d]	2.02	2.88	2.96	1.40	1.43	2.01
% SS formation[e]				80	79	99

[a] Expected number of sulfhydryl groups per protomer. [b] Expected number of intra-disulfide bonds per protomer. [c] Expected number of inter-disulfide bonds per protomer. [d] Measured number of sulfydryl groups per protomer. [e] Percentage of formation of designed disulfide bonds.

The recombinant proglycinin WT and mutants were purified by ion exchange and gel filtration column chromatography. All proteins were eluted at almost the same time on ion exchange column chromatography (data not shown), and elution times on gel filtration column chromatography were as follows: WT at 95.4 min, N116C at 95.4 min, P248C at 96.1 min, R161C at 95.4 min, F163C at 95.3 min, and N116C/P248C at 95.9 min. These results indicate that all mutant proteins fold correctly and assemble into a trimer like WT.

Confirmation of the Introduced Sulfhydryl Group and Disulfide Bond. To confirm whether the introduced cysteine residue is present as a free sulfhydryl group or forms a disulfide bond with a cysteine residue, we determined the number of sulfhydryl groups per protomer using DTNB (**Table 1**). The results showed that WT has two free cysteine residues as expected (*1*). The two mutants N116C and P248C designed to have three free cysteine residues were found to have three free cysteine residues. These results indicate that N116C and P248C contain an additional sulfhydryl group as compared with WT.

The two mutants R161C and F163C should have one sulfhydryl group per protomer, when the designed disulfide bond is completely formed with Cys377. As shown in **Table 1**, the number of sulfhydryl group for R161C and F163C was 1.40 and 1.43, respectively. These values correspond to 80 and 78% formation of the expected disulfide bond per protomer. In addition, N116C/P248C showed the same number of sulfhydryl group as that of WT, suggesting that the designed disulfide bond was completely formed between Cys116 and Cys248.

Since the formation of the disulfide bond was about 80% for R161C and F163C, dimer and trimer molecules should exist in the purified sample. Therefore, we checked the ratio of dimer and trimer by SDS−PAGE under nonreduced condition (**Figure 2**). Four kinds of molecules were found in the gel. The molecular sizes of the four bands were calculated at 52 000, 112 000, 150 000, and 200 000 on the basis of a standard curve, while only the band of 54 000 was observed on the SDS−PAGE gel under reduced conditions (data is not shown). Therefore, we defined the four molecules as monomer, dimer, trimer, and looped trimer, respectively, where the looped trimer includes three interprotomer disulfide bonds between Cys377 and Cys161

Table 2. Parameters for Stability and Kinetic Constants on α-Chymotrypsin Digestion

protein	WT	N116C	P248C	R161C	F163C	N116C•P248C
T_m (°C)[a]	75.3	76.2	75.7	75.9	79.0	80.1
C_m (M)[b]	3.38/0.02[c]	3.34/0.03	3.37/0.08	3.28/0.03	3.41/0.03	3.63/0.02
m (kcal/mol/M)[b]	2.35/0.25	2.74/0.39	2.18/0.43	3.03/0.37	3.66/0.21	2.41/0.38
$\Delta\Delta G$ (kcal/mol)[b]		1.2	–0.5	2.0	4.6	0.9
k_1 (%/min)[d]	3.8/0.3	3.2/0.1	3.6/0.2	4.9/0.2	4.2/0.1	2.0/0.2
k_2 (%/min)[d]	0.4/0.2	0.7/0.2	0.9/0.1	1.1/0.1	1.4/0.02	0.9/0.1

[a] Obtained from DSC experiment. [b] Parameters of chemical denaturation using guanidine hydrochloride. C_m is a concentration at which folded and unfolded molecules exist equivalently, m is a measure of the dependence on denaturant concentration, and $\Delta\Delta G$ is [$\Delta G(H_2O)$mutant – $\Delta G(H_2O)$WT]; $\Delta G(H_2O)$ is an estimate of the conformational stability of a protein at 0 M denaturant. [c] Standard error. [d] Kinetic constants of α-chymotrypsin digestion.

or Cys163 per proglycinin homotrimer, and the trimer includes two interprotomer disulfide bonds. Here, it is hypothesized that the looped trimer migrates more slowly than the trimer with two intersubunit disulfide bonds since their denatured structure should be different from each other. If the free energy of formation of a disulfide bond to form a dimer from two monomers is the same as that to form a trimer from a dimer or to form a looped trimer from a trimer, the ratios of existence of the monomer, dimer, trimer, and looped trimer are statistically calculated as 4.0, 6.4, 38.4, and 51.2%, respectively, based on the results by DTNB and binomial distribution. By densitometric analysis, ratios of existence of monomer and oligomers on R161C and F163C were measured as 7.0, 6.5, 24.0, and 62.5% and 17.1, 9.9, 27.7, and 45.3%, respectively. Although actual percentages of the looped trimer for R161C and the monomer for F163C were larger than their calculated values and those of trimer for both R161C and F163C were lower, the tendency of the measured value roughly corresponded to the calculated value. Thus, we conclude that 80% of introduced interprotomer disulfide bonds was successfully formed as determined using DTNB.

Structural Stability. The effect of engineered sulfhydryl groups and disulfide bonds on structural stability was evaluated by chemical and thermal denaturation experiments. In general, disulfide bonds could play an important role in the folding and the structural stability of a protein through the reduction of the number of conformations in the unfolded state (*24*, *25*). **Table 2** lists the parameters measured in this study. T_m is defined as the midpoint in the thermally induced transition from the folded to unfolded state. The double mutant N116C/P248C showed the highest T_m value, 4.8° higher than that of WT. This could be due to the intraprotomer disulfide bond formation. On the basis of the entropy change, the interprotomer disulfide bond should stabilize the protein structure more than the intraprotomer bond. However, the T_m value for F163C was 3.7° higher than that of WT, and the T_m value of R161C was similar to that of WT. Probably this is due to the destabilization brought about by the replacement of Arg161 and Phe163 with cysteine residue. Since both residues are buried in the protein molecule, the mutations result in a large cavity. The magnitude of their contribution in R161C and F163C is estimated to be 1.6 and 1.4 kcal/mol, respectively (*26*). In addition, Arg161 forms hydrogen-bonded salt bridge with Asp157 (**Figure 1**). As a result of the replacement of Arg161 with the cysteine residue, Asp157 loses its counterion inside the protein. This effect would account for R161C being thermally less stable than F163C.

Structural stability was also assessed by determining the chemical denaturation. Since the effect of the scan rate on T_m value was low (*27*), three values of C_m, m, and $\Delta\Delta G$ were calculated based on the linear extrapolation method by assuming a two-state mechanism (*19*, *20*), where $\Delta\Delta G$ is [$\Delta G(H_2O)$-mutant − $\Delta G(H_2O)$WT]. The C_m value of N116C/P248C was largest, and mutants of N116C and P248C showed a C_m value similar to that of WT. However, R161C and F163C did not show significantly higher C_m values such as the case of T_m value. This suggests that the stabilization effect of the interprotomer disulfide bond against thermal denaturation is greater than that against chemical denaturation.

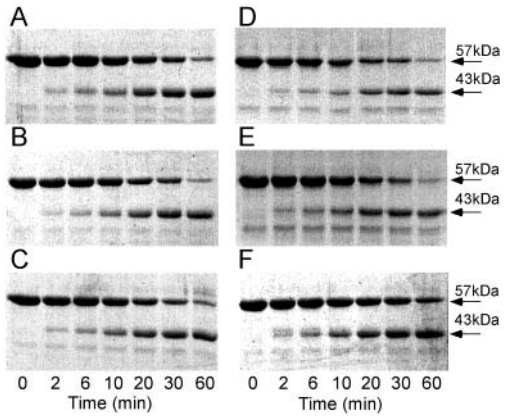

Figure 3. SDS–PAGE analysis of the digestibility of WT and mutant by α-chymotrypsin: (**A**) WT; (**B**) N116C; (**C**) P248C; (**D**) R161C; (**E**) F163C; (**F**) and N116C/P248C (1 μg of protein was loaded per well).

On the other hand, the m value shows the dependence of $\Delta G(H_2O)$ on denaturant concentration determined by the groups that are exposed to solvent in the denatured state (*20*). The increment of m value means that protein is unfolded to a greater extent than its WT (*28*). The m values for R161C and F163C are remarkably larger than that of WT. This indicates that R161C and F163C have a more extended structure than WT at the unfolded state. It is expected that the engineered interprotomer disulfide bonds will interfere in the formation of a denatured protein structure.

The $\Delta\Delta G$ of F163C was the highest in this study and that of R161C was significantly larger than that of N116C/P248C, indicating that both F163C and R161C mutants have a larger difference in free energy than WT between the folded and the unfolded states without chemical denaturant at 25 °C. The two mutants of F163C and R161C would be more stable than N116C/P248C under natural conditions but would be more sensitive to chemical denaturation. However, it appears that experimental error is not negligible because $\Delta G(H_2O)$ is calculated by extrapolation.

α-Chymotrypsin Digestion Analysis. To investigate whether the digestibility of mutants is different from that of WT, an experiment on α-chymotrypsin digestion was conducted (**Figure 3**). The kinetic constants k_1 and k_2 of α-chymotrypsin digestion are listed in **Table 2**. The cleavage site for the k_1 value is positioned at variable region II (*27*). N116C/P248C showed a significantly lower k_1 value than that of WT, although its k_2

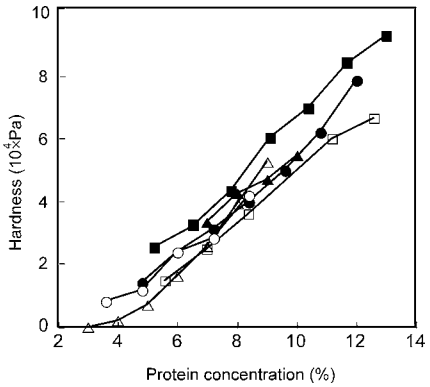

Figure 4. Heat-induced gelation. Unfilled square, WT; unfilled triangle, R161C; filled triangle, F163C; filled square, N116C/P248C; filled circle, N116C; and unfilled circle, P248C. Protein concentrations used for heating are indicated at horizontal axis. Averaged values of gel hardness were plotted.

value was slightly higher. On the other hand, k_1 values of R161C and F163C were higher than that of WT. These results suggest that R161C and F163C are destabilized under these conditions when compared with WT. It seems to be inconsistent with the result of $\Delta G(H_2O)$ on chemical denaturation. Perhaps the local conformation of R161C and F163C is different from that of WT around the cleavage site because the engineered residues in R161C and F163C are located near the variable region II.

Heat-Induced Gelation. Previously, we analyzed the functional properties and structural stabilities of recombinant proglycinin A1aB1b and its modified versions (*27*, *29*, *30*). The hardness of the heat-induced gel and the dependence on protein concentration of the WT proglycinin were similar to those of the native glycinin. Interestingly, the C12G mutant could not form a gel at protein concentration less than 5.6%, and the gel hardness of the C88S mutant was higher than that of native glycinin, while both mutants exhibited slight difference in structural stability. It is suggested that topology and number of sulfhydryl groups and disulfide bonds play an important role in heat-induced gelation.

Here, we measured the gel hardness of five mutants at various protein concentrations to investigate the effects of introduced SH groups and disulfide bonds. All mutants showed higher gel hardness than WT as expected (Figure 4), and it seems that the thermal stability of proglycinin does not correlate with gel hardness. Among the mutants, the hardness of N116C/P248C was the highest. Since only this double mutant has two more cysteine residues than WT, it appears that the hardness of the gel became higher according to an increased number of cysteine residue rather than because of the topological effect. However, all the mutations would be topologically efficient to increase the hardness of the gel since all introduced cysteine residues are designed to be located as far as possible from any endogeneous cysteine residues.

Since both native glycinin and recombinant proglycinin form transparent gels, their gelation process should be similar under the conditions examined here. On the basis of the model reported by Nakamura et al. (*11*), a particular unfolded-globular native glycinin molecule (partially unfolded but still globular) exists to some extent before the formation of strand I, which is a short strand consisting of about six glycinin molecules, and eventually longer strands and branched strands (strand III) could form a gel network. While the IA face will be interfaced for the formation of the strand I according to crystal structure and electron microscopy in the case of native glycinin (*6*, *11*), both IA and IE faces may be interfaced in the case of proglycinin (*5*). However, we cannot rule out the possibility that proglycinin may be assembled into a hexamer such as native glycinin at low ionic condition and high protein concentration before the gelation. Two replaced residues of Asn116 and Pro248 are located near the solvent not on the IA or IE face but on the side of the molecule, whereas Arg161 and Phe163 are buried in the protein. Therefore, we suggest that the two residues of Cys116 and Cys248 may particularly work during the formation of branched strands. On the other hand, the two residues of Cys161 and Cys163 could significantly contribute to network formation in gelation process because the interprotomer disulfide bond may function as a preexisting network between protomers. In fact, the *m* value by chemical denaturation indicated that R161C and F163C might have a different unfolded structure from WT.

Our study showed that the introduction of a new free SH residue and a new disulfide bond into soybean proglycinin is a powerful method to improve its heat-induced gel-forming ability. This could lead to the development of genetically modified soybean containing bioengineered glycinins with high gel-forming ability, which is suitable for food and industrial usage in the future.

ABBREVIATIONS USED

WT, recombinant wild-type proglycinin.

ACKNOWLEDGMENT

We thank Dr. E. M. T. Mendoza for her critical reading of the manuscript.

LITERATURE CITED

(1) Utsumi, S.; Matsumura, Y.; Mori, T. Structure−function relationships of soy proteins. In *Food Proteins and Their Applications*; Damodaran, S. Paraf, A., Eds.; Marcel Dekker: New York, 1997; pp 257−291.

(2) Nielsen, N. C.; Dickinson, C. D.; Cho, T.-J.; Thanh, V. H.; Scallon, B. J.; Fischer, R. L.; Sims, T. L.; Drews, G. N.; Goldberg, R. B. Characterization of the glycinin gene family in soybean. *Plant Cell* **1989**, *1*, 313−328.

(3) Dickinson, C. D.; Hussein, E. H. A.; Nielsen, N. C. Role of posttranslational cleavage in glycinin assembly. *Plant Cell* **1989**, *1*, 459−469.

(4) Utsumi, S. Plant food protein engineering. In *Advances in Food Nutrition Research 36*; Kinsella, J. E., Ed.; Academic Press: San Diego, CA, 1992; pp 89−208.

(5) Adachi, M.; Takenaka, Y.; Gidamis, A. B.; Mikami, B.; Utsumi, S. Crystal structure of soybean proglycinin A1aB1b homotrimer. *J. Mol. Biol.* **2001**, *305*, 291−305.

(6) Adachi, M.; Kanamori, J.; Masuda, T.; Yagasaki, K.; Kitamura, K.; Mikami, B.; Utsumi, S. Crystal structure of soybean 11S globulin: Glycinin A3B4 homohexamer. *Proc. Natl. Acad. Sci. U.S.A.* **2003**, *100*, 7395−7400.

(7) Wright, D. J. The seed globulins. In *Developments in Food Proteins*; Hudson, B. J. F., Ed.; Elsevier: London, 1987; Vol. 5, pp 81−157.

(8) Wright, D. J. The seed globulins. In *Developments in Food Proteins*; Hudson, B. J. F., Ed.; Elsevier: London, 1988; Vol. 6, pp 119−178.

(9) Mori, T.; Nakamura, T.; Utsumi, S. Gelation mechanism of soybean 11S globulin: formation of soluble aggregates as transient intermediates. *J. Food Sci.* **1982**, *47*, 26−30.

(10) Utsumi, S.; Nakamura, T.; Mori, T. A micromethod for measurements of gel properties of sybean 11S globulin. *Agric. Biol. Chem.* **1982**, *46*, 1923−1924.

(11) Nakamura, T.; Utsumi, S.; Mori, T. Network structure formation in thermally induced gelation of glycinin. *J. Agric. Food Chem.* **1984**, *32*, 349−352.
(12) Hermansson, A.-M. Structure of soya glycinin and conglycinin gels. *J. Sci. Food Agric.* **1985**, *36*, 822−832.
(13) Lee, S.-P.; Cho, Y.; Batt, C. A. Enhancing the gelation of β-lactoglobulin. *J. Agric. Food Chem.* **1993**, *41*, 1343−1348.
(14) Katsube, T.; Kurisaka, N.; Ogawa, M.; Maruyama, N.; Ohtsuka, R.; Utsumi, S.; Takaiwa, F. Accumulation of soybean glycinin and its assembly with the glutelins in rice. *Plant Physiol.* **1999**, *120*, 1063−74.
(15) Laemmli, U. K. Cleavage of structural protein during the assembly of the head of bacteriophage T4. *Nature* **1970**, *227*, 680−685.
(16) Ellman, G. L. Tissue sulfhydryl groups. *Arch. Biochem. Biophys.* **1959**, *82*, 70−77.
(17) Habee, A. F. S. A. Reaction of protein sulfhydryl groups with Ellman's reagent. *Methods Enzymol.* **1975**, *25*, 457−467.
(18) Bradford, M. M. A rapid and sensitive for the quatitation of microgram quantities of protein utilizing the principle of protein−dye binding. *Anal. Biochem.* **1976**, *72*, 248−254.
(19) Santro, M. M.; Bolen, D. W. Unfolding free energy changes determined by the linear extrapolation method. 1. Unfolding of phenylmethanesulfonyl α-chymotrypsin using different denaturants. *Biochemistry* **1988**, *27*, 8063−8068.
(20) Pace, C. N.; Shaw, K. L. Linear extrapolation method of analyzing solvent denaturation curves. *Proteins* **2000**, *4*, 1−7.
(21) Shrager, R. I.; Mihalyi, E.; Towne, D. W. Proteolytic fragmentation of fibrinogen. II. Kinetic modeling of the digestion of human and bovine fibrinogen by plasmin or trypsin. *Biochemistry* **1976**, *15*, 5382−5386.
(22) Hazes, B.; Dijkstra, B. W. Model building of disulfide bonds in proteins with known three-dimensional structure. *Protein Eng.* **1988**, *2*, 119−125.
(23) Thornton, J. M. Disulphide bridges in globular proteins. *J. Mol. Biol.* **1981**, *151*, 261−287.
(24) Fersht, A. R.; Serrano, L. Principles of protein stability derived from protein engineering experiments. *Curr. Opin. Struct. Biol.* **1993**, *3*, 75−83.
(25) Bonander, N.; Leckner, J.; Guo, H.; Karlsson, B. G.; Sjölin, L.; Crystal structure of the disulfide bond-deficient azurin mutant C3A/C26A. *Eur. J. Biochem.* **2000**, *267*, 4511−4519.
(26) Chakravarty, S.; Bhinge, A.; Varadarajan, R. A procedure for detection and quantitation of cavity volume in protein. *J. Biol. Chem.* **2002**, *277*, 31345−31353.
(27) Adachi, M.; Okuda, E.; Kaneda, Y.; Hashimoto, A.; Shutov, A. D.; Becker, C.; Muntz, K.; Utsumi, S. Crystal structures and structural stabilities of the disulfide bond-deficient soybean proglycinin mutants C12G and C88S. *J. Agric. Food Chem.* **2003**, *51*, 4633−4639.
(28) Myers, J. K.; Pace, C. N.; Scholts, J. M. Denaturant *m* values and heat capacity changes: relation to changes in accessible surface areas of protein unfolding. *Protein Sci.* **1995**, *4*, 2138−2148.
(29) Kim, C.-S.; Kamiya, Y.; Sato, S.; Utsumi, S.; Kito, M. Improvement of nutritional value and functional properties of soybean glycinin by protein engineering. *Protein Eng.* **1990**, *3*, 725−731.
(30) Utsumi, S.; Gidamis, A. B.; Kanamori, I.; Kang, I. J. Kito, M. Effects of deletion of disulfide bonds by protein engineering on the conformation and functional properties of soybean proglycinin. *J. Agric. Food Chem.* **1993**, *41*, 687−691.
(31) Kraulis, P. MOLSCRIPT—a program to produce both detailed and schematic plots of protein structures. *J. Appl. Crystallogr.* **1991**, *24*, 946−950.
(32) Meritt, E. A.; Murphy, M. E. P. Raster3D version 2.0, a program for photorealistic molecular graphics. *Acta Crystallogr., Sect. D* **1994**, *50*, 869−873.

Received for review February 29, 2004. Revised manuscript received June 14, 2004. Accepted July 1, 2004. This work was supported in part by a grant to M.A. and S.U. from the Ministry of Education, Science and Culture of Japan.

JF0496595